

Ultracompact, low-loss directional couplers on InP based on self-imaging by multimode interference

E. C. M. Pennings, R. J. Deri, A. Scherer, R. Bhat, T. R. Hayes,^{a)} N. C. Andreadakis, M. K. Smit,^{b)} L. B. Soldano,^{b)} and R. J. Hawkins^{c)}
Bellcore, 331 Newman Springs Road, Red Bank, New Jersey 07701-7040

(Received 12 June 1991; accepted for publication 12 August 1991)

We report extremely compact (494- μm -long 3 dB splitters, including input/output bends), polarization-insensitive, zero-gap directional couplers on InP with a highly multimode interference region that are based on the self-imaging effect. We measured cross-state extinctions better than 28 dB and on-chip insertion losses of 0.5 dB/coupler plus 1 dB/cm guide propagation loss at 1523 nm wavelength.

Directional couplers are key components in integrated optoelectronics, being used in power dividers, modulators and switches, wavelength (de)multiplexers, and polarization splitters. Their major drawback for monolithic integration is their large size, typically several millimeters or more, due to large coupling lengths and due to the size of the branching network that separates the access waveguides.¹ The zero-gap two-mode interference coupler has a much shorter coupling length than the conventional synchronous directional coupler, but it cannot be used in conjunction with deeply etched waveguides that are suitable for very compact monomode bends.² In particular, the abrupt branching guide-to-coupler transitions resulting from the large index differences required for compact bends can degrade coupler crosstalk.³ Here we demonstrate that high extinction and compact size can be achieved by combining deeply etched monomode guides for compact bends with zero-gap, multimode interference (MMI) couplers. Such couplers have previously been proposed for easing the fabrication of zero-gap couplers by eliminating the need for well-defined Y junctions;⁴ here we show that MMI couplers are suitable for high extinction (typically 28 dB), polarization-insensitive, compact (sub-millimeter) devices with low on-chip insertion loss.

The self-imaging effect which occurs in the multimode interference region of our coupler is crucial to our design (Fig. 1). Such self-imaging has been reported by Ulrich⁵: in a multimode waveguide of length $L = (p/q)3L_\pi$ where L_π is the beat length for the two lowest-order modes, the input field is imaged onto the output when $(p/q) = 2, 4, \dots$. A reverse image is produced at the output for $(p/q) = 1, 3, \dots$ and likewise a linear combination of the image and its reverse occur when $(p/q) = 1/2, 3/2, \dots$. At these lengths, a super-resonance occurs in which *all* excited modes interfere constructively. Consequently, the coupler operates independently of its excitation, thus permitting the use of deeply etched waveguides for the input and output branching network. These waveguides combine monomode operation with short radii of curvature. The independence of excitation also allows the input waveguides to be

spaced far apart (we employed a 2.4 μm separation between the access waveguides). Increasing the distance between the access waveguides reduces problems, as associated with the photolithographic definition of the Y junction, it leads to a large extinction ratio in the cross state and it eliminates the radiation loss associated with coupling between the bends in the branching network. In addition, we expect the self-imaging effect to be polarization insensitive. Using self-imaging, lossless couplers are only achievable for cross-, bar-, and 3 dB-power splitting. These splitting ratios are sufficient for most applications, however, such as switches, star couplers, and as 3 dB combiners in balanced coherent receivers. While it is possible to design couplers operating at lengths based on multiples of L_π (rather than $3L_\pi$) by positioning input guides to avoid excitation of certain coupler modes,⁴ we employ here structures which *only* function at $3L_\pi$, not at L_π . While the $3L_\pi$ design appears to increase the required coupler length over the L_π device, constraints on input positioning lead to a wider coupler with longer beat length in the L_π design. Our calculations show that both approaches lead to comparable coupler lengths; we employed here devices with an interference section of nominal 8 μm (actual 7.7 μm) width and four guided modes, which leads to interference section

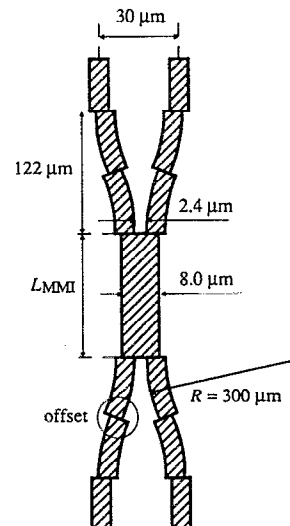


FIG. 1. Schematic layout of the multimode interference coupler.

^{a)}AT&T Bell Laboratories, 600 Mountain Avenue, Murray Hill, NJ 07974.

^{b)}Department of Electrical Engineering, Delft University of Technology, 2600 GA Delft, The Netherlands.

^{c)}Lawrence Livermore National Laboratory, Livermore, CA 94550.

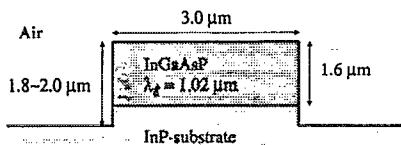


FIG. 2. Waveguide cross section. The fabricated waveguide has an actual width $w \approx 2.7 \mu\text{m}$.

lengths of 250 or 500 μm for the 3 dB or cross states, respectively.

Our waveguides are conventional, single-mode InGaAsP ($\lambda_g = 1.02 \mu\text{m}$)/InP single heterostructures (Fig. 2) grown by low-pressure organometallic chemical vapor deposition, with ribs etched through the InGaAsP cores for compact bend performances. Rib fabrication was formed by dry etching through a resist mask using either Cl_2/Xe^+ chemically assisted ion beam etching (CAIBE)⁶ or CH_4/H_2 reactive ion etching (RIE).⁷ Straight guide propagation losses were 0.8–1.1 dB/cm and 2.2 dB/cm for CAIBE and RIE fabrication, respectively, as determined from Fabry–Pérot measurements on different guide lengths using $\lambda_0 = 1523 \text{ nm}$ wavelength, TE-polarized light (facet power reflectivity $r \approx 0.283$). The losses obtained with RIE are comparable to the best values reported for dry-etched guides with deep ribs,² those obtained with CAIBE are a factor of 2 lower than the best dry-etch values and are comparable to the best results obtained for deep-rib guides using wet chemical etching.²

We conservatively employ circular bends of $R = 300 \mu\text{m}$ radius (simulations⁸ suggest $R = 200 \mu\text{m}$ suffices for low loss). Using this radius of curvature, the total branching network (in-plus output) is only 244 μm long for a 30 μm waveguide separation. The total device lengths (coupler plus branching) are 494 μm (3 dB) and 744 (cross). Due to our compact bend radii, devices with larger input/output guide separation (125 μm) will remain quite compact: only 772 μm for the 3 dB coupler. Lateral offsets have been used in order to minimize transition losses due to mode mismatch at the junction of two oppositely curved bends or at a junction of a bend and a straight waveguide.^{9,10} The Fabry–Pérot and transmission techniques were used to evaluate the excess bend loss with respect to straight reference waveguides on the same chip. An excess bend loss of only 0.3 dB was found at $\lambda_0 = 1523 \text{ nm}$ for the total branching network (in-plus output) for both polarizations which is in close agreement with the predicted value of 0.32 dB. This calculated loss value consists of transition losses at the junctions only (the radiation loss is very small because of the large horizontal refractive-index difference) and has been evaluated by means of one-dimensional overlap integrals.

We fabricated a series of passive couplers of differing lengths, all on a single chip, with *S*-bend input/output branching as described above. Scanning electron microscopy (SEM) micrographs (Fig. 3) of the resulting devices show smooth sidewalls for low scattering loss and well-defined gaps between input guides. After antireflection



FIG. 3. Scanning electron micrograph of a coupler fabricated by chemically assisted ion beam etching.

coating of endfacets with SiO ($r \approx 0.01$) to avoid Fabry–Pérot effects, devices were characterized by transmission measurements using $\lambda_0 = 1523 \text{ nm}$ light and microscope objective input/output coupling. On-chip insertion loss was measured relative to straight reference guides and *S* bends without couplers on the same chip. The measured dependence of power splitting and loss on coupler interference length agrees well with simulations, as shown in Fig. 4 for $\lambda_0 = 1523 \text{ nm}$, TE polarization, and devices etched by RIE. Both simulated and experimental values in this figure

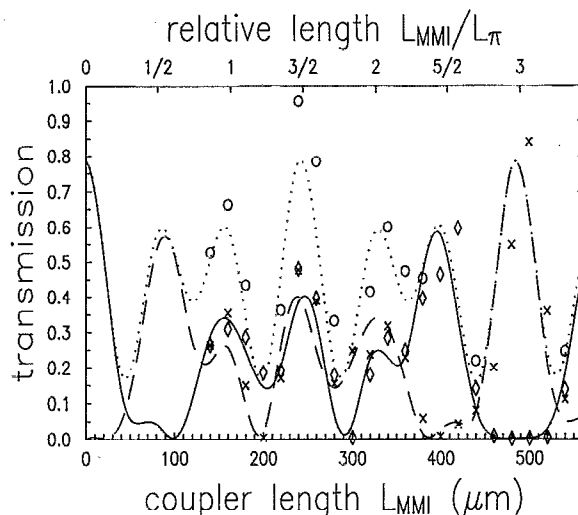


FIG. 4. Dependence of the coupler transmission on the length of the interference section. The output of each port (output on same side as input; solid curve, diamonds; output and input on opposite sides; dashed curve and crosses) and the sum total of both outputs (dotted curve and circles) are shown. The curves represent calculated performance, and the discrete markers show experimental results for a series of devices on the same chip which was fabricated using reactive ion etching. Unity transmission corresponds to the insertion loss of a straight reference waveguide. Upper scale shows the coupler length normalized by the beat length L_π .

include *S*-bend losses. We obtain a splitting ratio of 49.8:50.2 for the 3 dB state (coupler length 240 μm) and 27.6 dB extinction for the cross state (500 μm coupler length). Our best measured value of the extinction ratio is 33 dB. The insertion losses of these devices were 0.4–0.7 dB with respect to straight reference guides. These values include *S*-bend/branching losses, indicating that the couplers themselves exhibit low losses (<0.4 dB). The measured insertion losses appear to be somewhat smaller than those predicted theoretically, which we tentatively attribute to a possible contribution of a fifth guided or leaky mode in the interference section. The presence of a leaky mode would also explain why the discrepancy between the measured and the observed insertion loss is larger for the 3 dB state than for the cross state (Fig. 4). Similar coupler performance has been observed on separately processed chips using CAIBE for rib etching. Thus, our results demonstrate that multimode interference couplers can be used with deeply etched rib guides to achieve submillimeter devices (including *S* bends) with high extinction and low insertion loss. Our data (Fig. 4) also present a clear demonstration of the super-resonance phenomenon in self-imaging: while low-loss 3 dB and cross states are achieved at lengths $3L_\pi/2$ and $3L_\pi$, poor crosstalk and insertion loss occur at lengths $L_\pi/2$ and L_π associated with conventional couplers.

For many applications, acceptable tolerances in device fabrication and operating conditions are as important as optimal device performance itself. Changes in device performance due to fabrication errors (coupler width w or length L) or operating conditions (λ_0 , polarization, temperature) can be deduced from transmission versus L curves (Fig. 4) and the formula for $3L_\pi \approx 4Nw^2/\lambda_0$, where N is the slab guide effective index in the coupler. For example, our data indicate that a $\pm 4\%$ change in L_π results in a splitting ratio better than 49:51 and additional loss ≤ 0.8 dB for 3 dB couplers. This change corresponds to a wavelength range > 100 nm, or fabrication errors of ± 0.2 μm in width or ± 10 μm in length. In order to assess the insensitivity of the couplers to operating conditions, the 3 dB state and the cross-state couplers have been measured at a temperature of 70 $^\circ\text{C}$ ($\lambda_0 = 1523$ nm) and at $\lambda_0 = 1540$ nm (room temperature) using a semiconductor laser and fiber excitation. These measurements revealed no significant change in behavior; the total insertion losses remain below 0.5 dB, the 3 dB splitters show splitting ratios better than 49:51 and the cross-state couplers have an extinction ratio better than 27 dB. Experiments with TM polarization at $\lambda_0 = 1523$ nm show essentially no change in

behavior for the same couplers (240, 500 μm lengths) described above: 49.9:50.1 splitting ratio and 0.5 dB loss for 3 dB splitters and 28.4 dB extinction and 0.6 dB loss in the cross state. The devices are polarization insensitive, but not polarization independent, in that the optimal crosstalk is achieved for devices of somewhat different length (31.2 dB at 480 μm length for TE polarization and 33.3 dB at 520 μm length for TM polarization).

In conclusion, we have shown that ultracompact directional couplers with high performance (high extinction, low insertion loss, low polarization sensitivity) can be realized by taking advantage of the self-imaging effect in multimode interference structures. This work can lead to an entire class of ultracompact integrated optic devices based on such couplers. For example, combining our coupler structures with previously demonstrated compact phase shifters¹¹ should create switching devices in which the input/output branching, as well as the interaction region, are extremely compact. Replacing our *S*-bend structures with integrated mirrors (of the type described in Ref. 12) will achieve even shorter devices, at the expense of increased branching insertion loss. The self-imaging in our couplers permits operation with multimode input/output guides, which can improve mirror losses.

We acknowledge useful conversations and technical assistance from L. M. Schiavone. This work was supported in part under the auspices of the U.S. Department of Energy under contract No. W-7405-ENG-48.

¹H. Inoue, K. Hiruma, K. Ishida, H. Sato, and H. Matsumura, *Appl. Opt.* **25**, 1484 (1986).

²M. Seto, R. J. Deri, A. Yi-Yan, E. Colas, W. J. Tomlinson, R. Bhat, and A. Shahar, *J. Lightwave Technol.* **LT-8**, 264 (1990).

³H. A. Haus and N. A. Whitaker, Jr., *Appl. Phys. Lett.* **46**, 1 (1985).

⁴L. B. Soldano, F. B. Veerman, M. K. Smit, B. H. Verbeek, and E. C. M. Pennings, *Technical Digest Integrated Photonics Research* (Optical Society of America, Washington, DC, 1991), Paper TuD1, p. 13.

⁵R. Ulrich and G. Ankele, *Appl. Phys. Lett.* **27**, 337 (1973).

⁶A. Scherer, J. L. Jewell, Y. H. Lee, J. P. Harbison, and L. T. Florez, *Appl. Phys. Lett.* **55**, 2724 (1989).

⁷T. R. Hayes, P. A. Heimann, V. M. Donnelly, and K. E. Strege, *Appl. Phys. Lett.* **57**, 2817 (1990).

⁸E. C. M. Pennings and R. J. Deri, *Technical Digest Integrated Photonics Research* (Optical Society of America, Washington, DC, 1991), Paper ThF1, p. 107.

⁹E.-G. Neumann, *IEE Proc. Pt. H* **129**, 278 (1982).

¹⁰B. H. Verbeek, E. C. Pennings, J. W. M. van Uffelen, and P. J. A. Thijs, *Proceedings of the 15th European Conference on Optical Communications*, Gothenburg, Sweden, 1989, Paper PDB-9, p. 78.

¹¹J. E. Zucker, M. Wegener, K. L. Jones, T. Y. Chang, N. Sauer, and D. S. Chemla, *Appl. Phys. Lett.* **56**, 1951 (1990).

¹²P. Albrecht, W. Döldissen, U. Niggebrügge, H.-P. Nolting, and H. Schmid, *Proceedings of the 14th European Conference on Optical Communications*, Brighton, U.K., 1988, p. 235.